The Douglas-Rachford method for finding intersections of hypersurfaces

Jonathan M. Borwein, Scott B. Lindstrom, Brailey Sims, Matt Skerrit
CARMA, University of Newcastle, Callaghan, Australia
Anna Schneider, Universität der Bundeswehr, München

Splitting Algorithms, Modern Operator Theory, and Applications, Casa Matematica Oaxaca 2017
Last Revised September 15, 2017

https://www.carma.newcastle.edu.au/scott/

60th annual meeting
2016 — Canberra

Outline I

Definitions

- Let H be a Hilbert space
- The projection onto a nonempty closed subset C is given by

$$P_C(x) := \left\{ z \in C : \|x - z\| = \inf_{z' \in C} \|x - z'\| \right\}.$$

- When C is convex the projection operator P_C is single valued.
- The reflection mapping R_C is defined by

$$R_C := 2P_C - I,$$

where I is the identity.

Construction

Definition

Given two closed sets A and B, and an initial point $x_0 \in H$, the Douglas-Rachford method generates a sequence $(x_n)_{n=1}^{\infty}$ as follows:

$$x_{n+1} \in T_{A,B}(x_n) \quad \text{where} \quad T_{A,B} := \frac{1}{2}\left(I + R_B R_A\right). \tag{1}$$

- When the two sets A and B are clear from the context we will simply write T instead of $T_{A,B}$.
- The process may be concisely described as "reflect across A, reflect across B, average with start."

"Sometimes it is easier to see than to say." — Jon Borwein

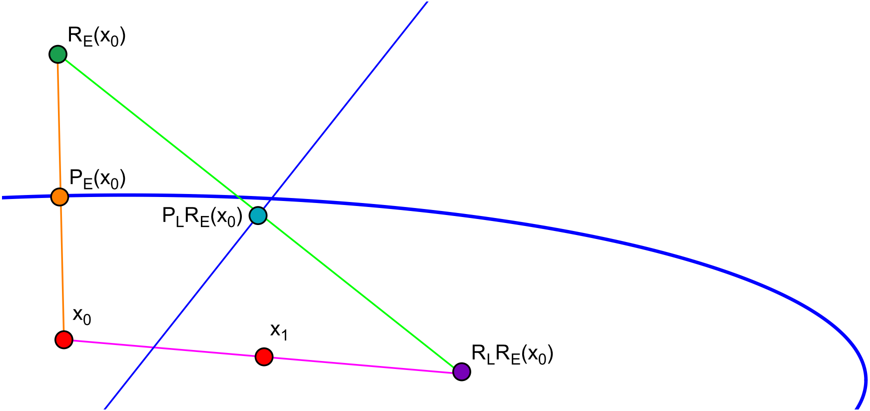

Figure: One iterate of Douglas-Rachford Method $T_{E,L}$

The Classical Result

Theorem (Lions-Mercier, 1979)

Suppose $A, B \subseteq H$ are closed and convex with non-empty intersection. Given $x_0 \in H$ the sequence defined by

$$x_{n+1} := T_{A,B}x_n \quad \textit{where} \quad T_{A,B} := \frac{1}{2}(I + R_B R_A)$$

converges weakly to an $x \in \mathrm{Fix} T_{A,B}$ with $P_A x \in A \cap B$.

(with original monotone sum of operators condition relaxed by Bauschke, Luke, Combettes in [7])

Circle and Line

Where the sets are the 2-sphere and a line, global convergence except on a singular manifold (the subspace orthogonal to the line) was first hypothesized by Borwein and Sims [12] and later proven by Benoist[9].

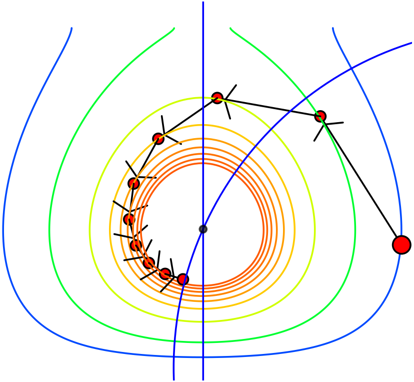

Figure: A Cinderella Script shows the Douglas Rachford algorithm for the 2-sphere and line along with the level sets for the Lyapunov function from Benoist's paper [9].

Generalizing from the Circle

The 2-sphere is a specific case of two more general kinds of sets, namely:

- Ellipses satisfying

$$E := \{(u,v) \in \mathbb{R}^2 | \left(\frac{u}{a}\right)^2 + \left(\frac{v}{b}\right)^2 = R^2\} \text{ for fixed } a, b, R. \quad (2)$$

- p-Spheres satisfying

$$S := \{(u,v) \in \mathbb{R}^2 | (u)^p + (v)^p = R^2\} \text{ for fixed } R. \quad (3)$$

Experimental Discovery

- Projection onto the 2-sphere is simple; for any x: $(P_S(x) = x/||x||)$.
- Projection for ellipses and p-spheres, by contrast, is not simple.
- We built customized numerical solvers and used Cinderella to explore the behavior dynamically
- Because the projections are far more complicated, a Lyapunov proof similar to that for the 2-sphere seemed unlikely
- Study with Cinderella revealed — and we subsequently proved — that convergence holds only locally; the singular set becomes more complicated.
- In the absence of an explicit proof, we turned to parallelization to better study convergence

Dynamic Discoveries!

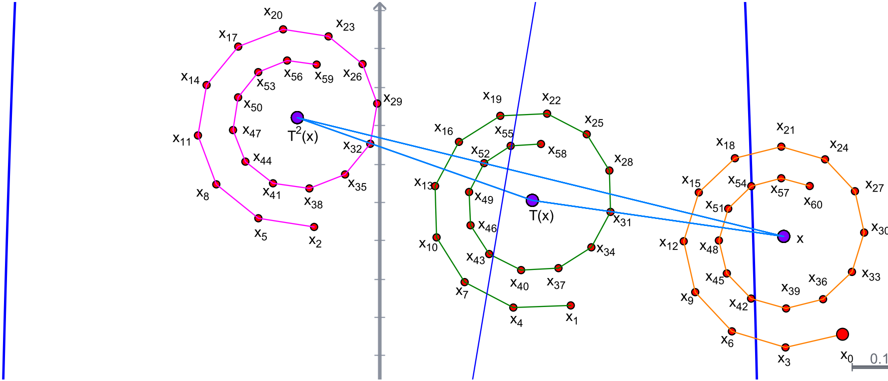

Figure: Period 3 points and corresponding basins of attraction for an ellipse and line.

p-Spheres

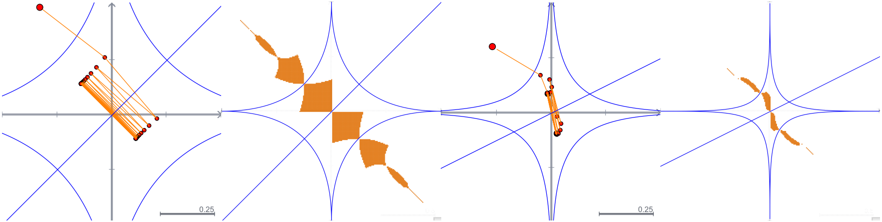

Figure: Left: for the 1/2-sphere, a singular manifold of period 2 points appears with basins of attraction (or "periodic attraction" rather). Right: for the 1/3-sphere, a pair of period 2 points appears with basins of attraction.

Ellipses

- The situation becomes even more interesting in the case of the Ellipse.
- As the Ellipse is stretched (as b grows), periodic points begin to appear.
- Points of greater period seem to appear with more stretching of the Ellipse.
- We chose to examine in detail the ellipse $b = 8$ and line through the origin of slope 6.

$b = 8$ Ellipse, $y = 6x$ Line

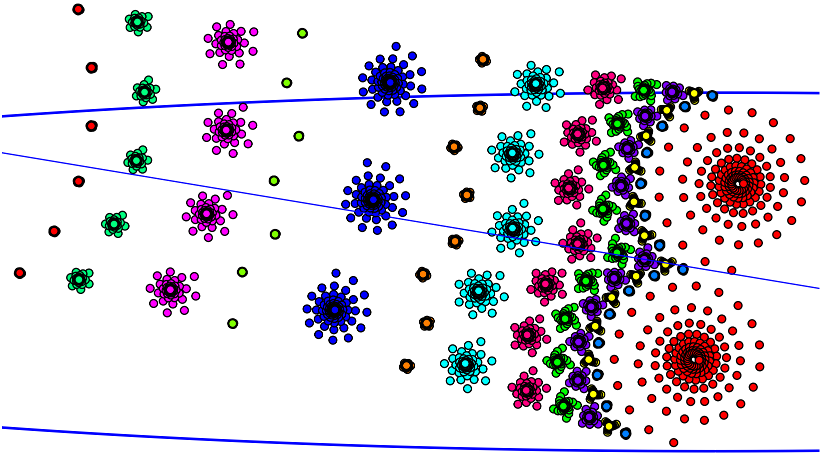

Figure: Points of periodicity appear with basins of attraction.

Basins

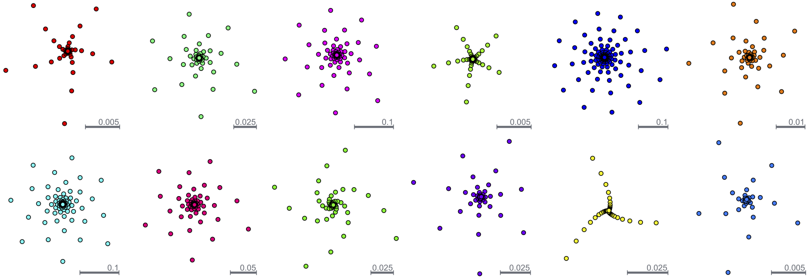

Figure: One spiral is shown from each of the sets of periodic points except for the period 2 points (which are already easily visible in the previous slide). The colors are exactly as they were in the previous slide.

Attractive and Repelling Basins

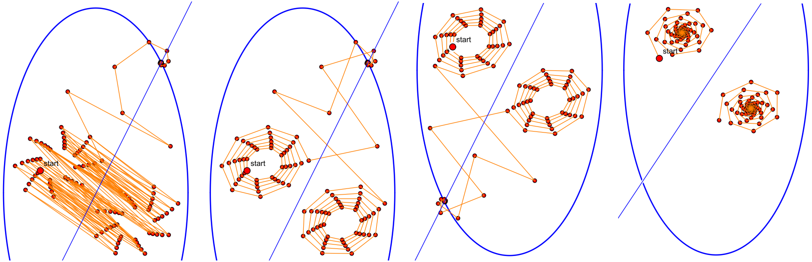

Figure: Far Left: for the $b = 2$ ellipse, the line $y = 2x$ yields period two points which are unstable. Center Left: we connect every second iterate. Center Right: a tiny perturbation of the starting point determines which feasible point iterates go to. Far Right: rotating the line, periodic points also rotate and become stable.

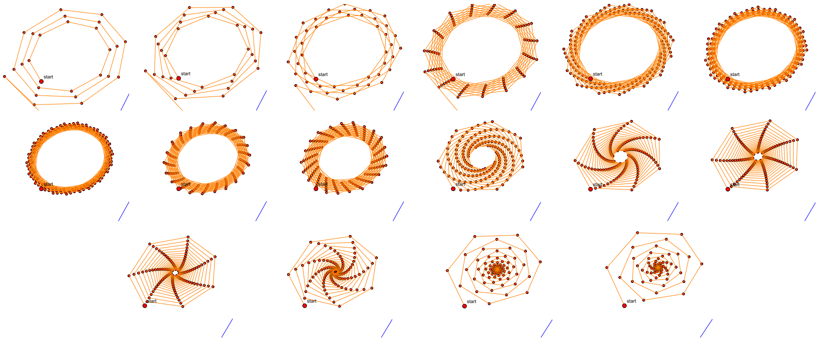

Figure: We connect Every second iterate for the $b = 2$ ellipse with 300 iterates. We start at upper left with the line $y = 2x$ and rotate it further in each frame until we have the line $y = \frac{3}{2}x$ at bottom right. Part of the line is visible in the bottom right corner of each frame. As we rotate the line, we see the speed at which iterates escape from the source basin decreases until eventually the source basin turns into a sink basin.

The Role of Parallelization

- To visualize the regions of convergence, we attempted to create potential Lyapunov curves numerically.
- This requires numerical inversion of Douglas Rachford.
- We first attempted this for the 2-sphere whose explicit Lyapunov function is known
  - Even for the 2-sphere, the induced functions behave poorly and *Maple*'s built-in root-finders struggled.
  - For any ellipse with $b \neq 1$, numerical inversion is even more unreliable.
- This led us to use parallelization

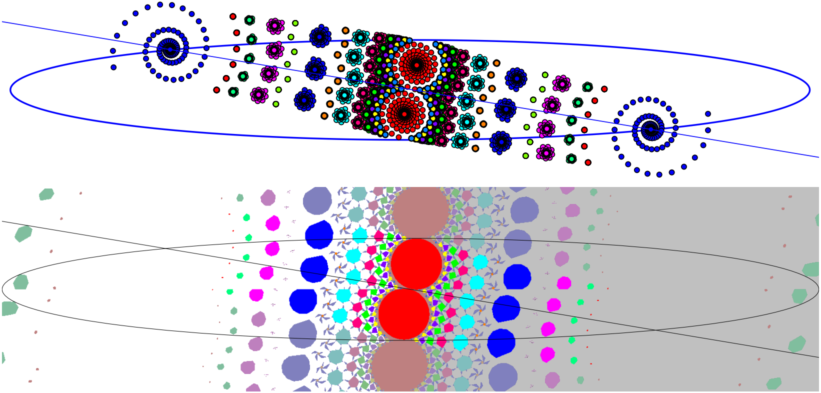

Figure: The $b = 8$ ellipse and $y = 6x$ line with both Cinderella plot and plot of the basins.

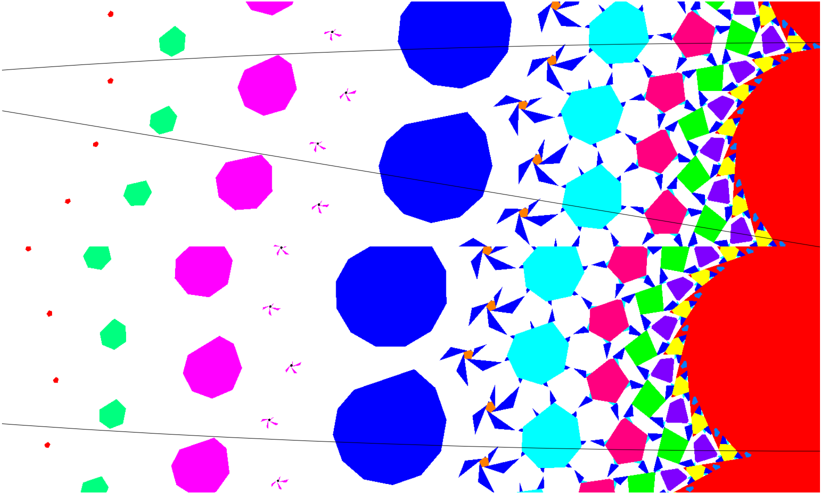

Figure: Zoomed in on the basins.

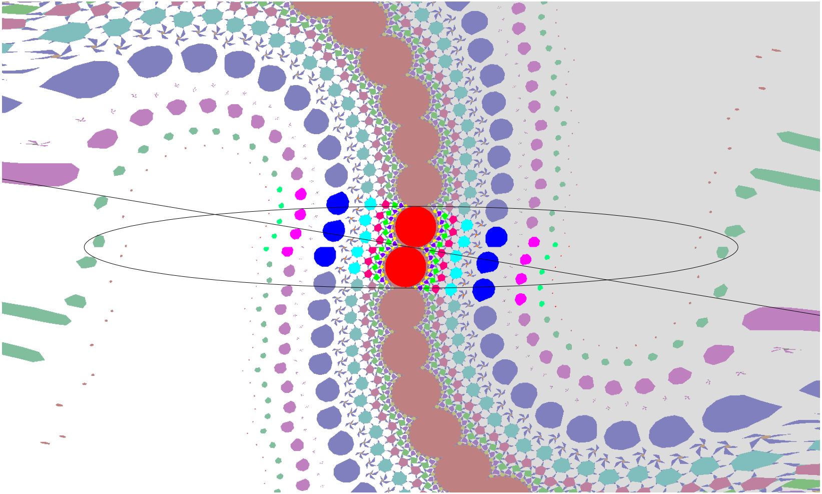

Figure: Zoomed out to see the regions around the ellipse.

MoCaO Poster Image Version

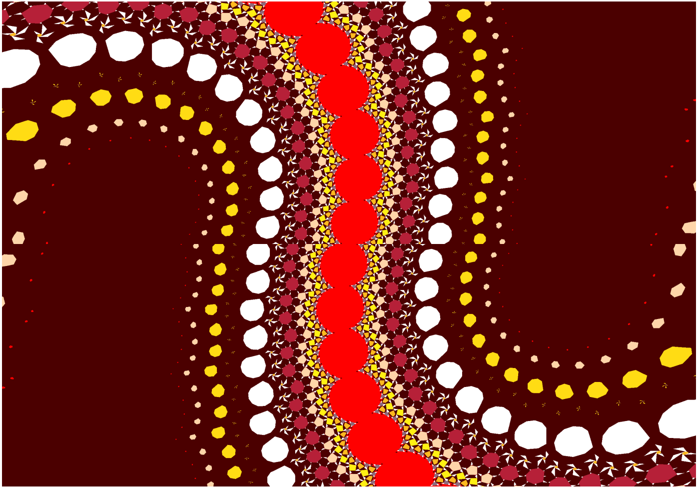

Figure: Coloring based on indigenous Australian art.

Numerical Accuracy

- In our follow-up paper, "Computing Intersections of Implicitly Specified Plane Curves," [22] we explored Douglas-Rachford with Euclidean reflection replaced by Schwarzian Reflection.
- We also created a new projection by computing the intersection of the curve with the line through the point and its Schwarzian reflection.
- Observed deviation of this new method from Euclidean reflection computed by solving Lagrangian system was negligible.

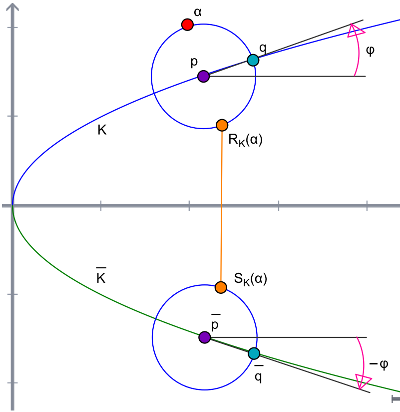

Figure: Schwarzian Reflection

Lessons about Convergence and Behavior

We compare observations about ellipses to experimental results using Douglas-Rachford by Aragón, Borwein, and Tam.

5	3			7				
6			1	9	5			
	9	8					6	
8				6				3
4			8		3			1
7				2				6
	6					2	8	
			4	1	9			5
				8			7	9

Figure: Solving sudoku puzzles [2].
Image source Wikimedia Commons [25]

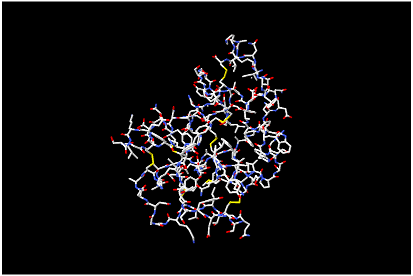

Figure: Solving incomplete euclidean distance matrices for protein mapping [3] [14], see also Borwein and Bailey [5].

Convergence: Sudoku 1

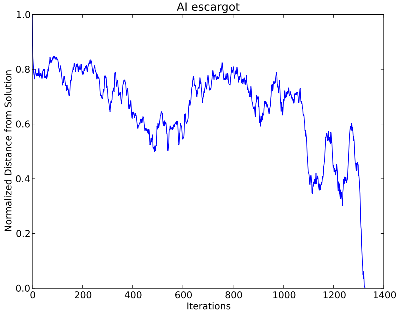

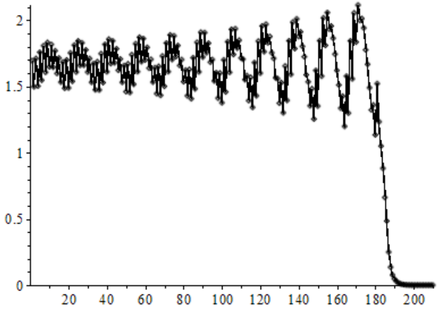

Figure: Left: distance to the solution by iterations of Douglas Rachford for a sudoku puzzle. Right: for the $b = 2$ ellipse with line $y = 2x$ with 210 iterates, distance from each iterate to the particular feasible point the sequence converges to.

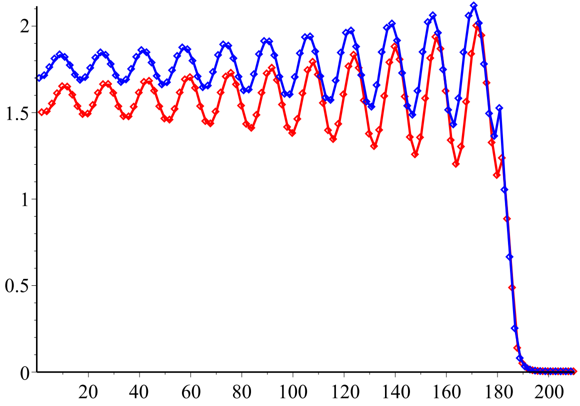

Figure: The same iterates from the right side are shown. By connecting every second iterate and color-coding, we see subsequences in the two different source basins.

Convergence: Sudoku 2

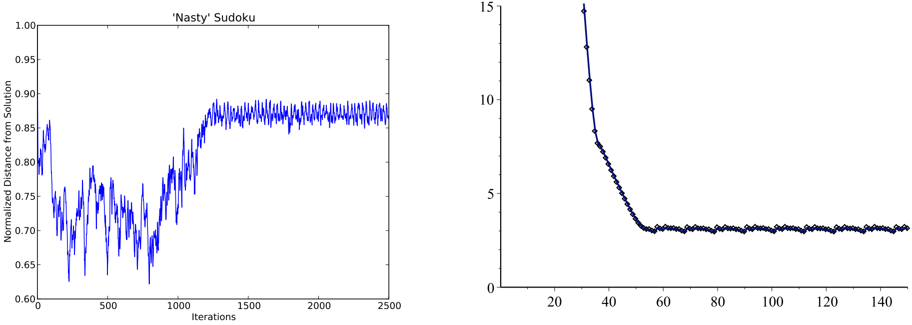

Figure: Left: distance to the solution by iterations of Douglas Rachford for a sudoku puzzle. Right: 150 iterates for the $b = 14$ ellipse and line $y = 9x$. The iterates approach the ellipse before being pulled into the attractive basins for period 11 points.

Matrix Completion: EDMs

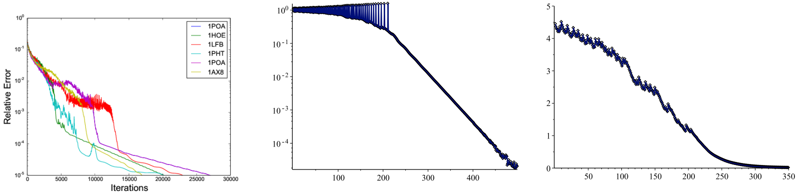

Figure: Left: relative error by iterations (Vertical axis logarithmic) for the Euclidean distance matrices for five proteins. Center: for the $b = 8$ ellipse and line $y = 6x$, relative error by iterations (vertical axis logarithmic) for the 300 iterates which are pictured in Figure 20. Right: distance to the actual feasible point for the same 300 iterates.

When Convergence is Slow: Ellipse

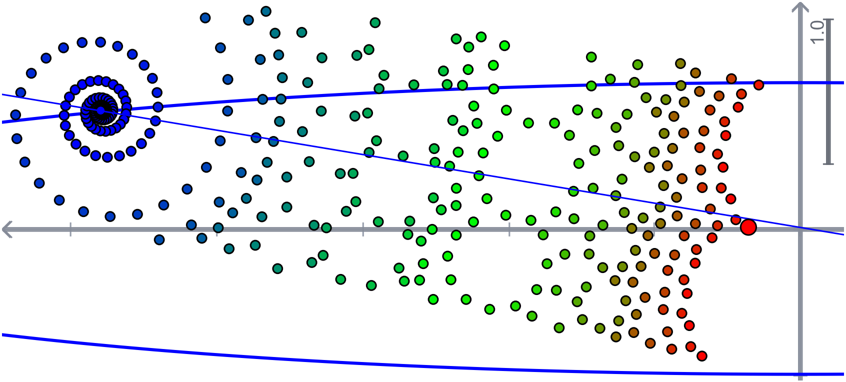

Figure: For the $b = 8$ ellipse and the line $y = 6x$, convergent sequences of iterates started among the basins of periodicity appear to trace out the shape of the basins on their way to the feasible point.

A Result on Infeasibility

Theorem

In a Euclidean Space X, let A, B be sets. Further suppose one of the following:

1. *A is compact and $\mathrm{co}(A)$ and $\mathrm{cl}(\mathrm{co}(B))$ are disjoint.*
2. *B is compact and $\mathrm{cl}(\mathrm{co}(A))$ and $\mathrm{co}(B)$ are disjoint.*

Then, where x_0 is the starting point and $\{x_n\}_{n=1}^{\infty}$ are the iterates for Douglas Rachford $T_{A,B}$, we have that $||x_n||$ tends linearly to ∞ with a step size of at least $d(A, B)$.

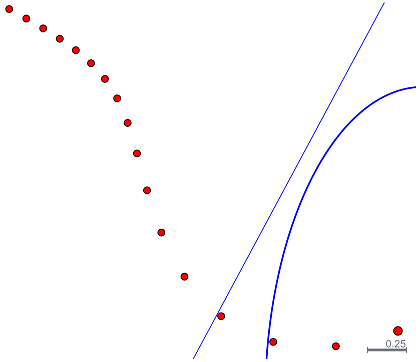

Figure: Divergence Theorem is illustrated

A Result on Infeasibility

Corollary

The image also illustrates a corollary. Using a result from Bauschke and Moursi [8], the purple shadow sequence converges to the point on the ellipse which is nearest the line.

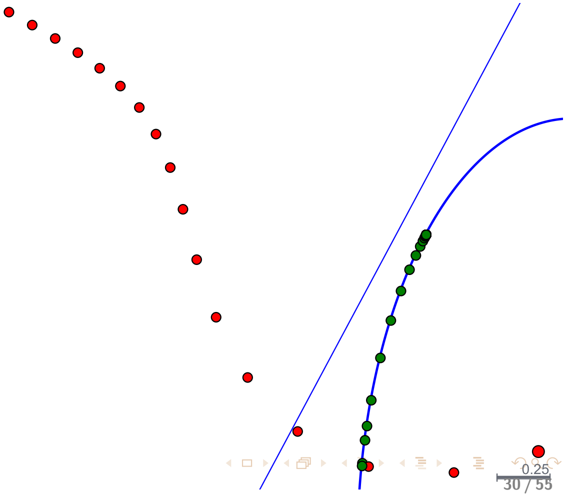

Extension to Many Sets

- We can apply this method to a feasibility problem with N sets $\Omega_1 \dots \Omega_N$ to find $x \in \cap_{k=1}^{N} \Omega_k$.
- We do so by working in the product space X^N as follows:
  - $A := \Omega_1 \times \cdots \times \Omega_N$
  - $B := \{x = (x_1, \dots, x_N) | x_1 = x_2 = \cdots = x_N\}$
- We call this the "divide and concur" method.
  - A is "divide" step of pointwise projection onto the individual sets from the feasibility problem.
  - B is "concur" step of projection onto the set of agreement.

Boundary Valued ODEs

- Consider the problem

$$y'' = f(y', y, t) \text{ for } a \le t \le b \text{ with } y(a) = \alpha, y(b) = \beta$$

- Using the finite differences method, we can reformulate a numerical ODE problem as a feasibility problem.
- Let $t_1 \dots t_N$ be interior mesh points, so we are computing with $N+1$ segments $[a, t_1], [t_1, t_2], \dots, [t_N, b]$ of length h.
- By an appropriate centered difference formula,

$$\frac{y(t_{i+1}) - 2y(t_i) + y(t_{i-1})}{h^2} = f\left(t_i, y(t_i), \frac{y(t_{i+1}) - y(t_{i-1})}{2h} - \frac{h^2}{6} y'''(\eta)\right) + \frac{h^2}{12} y^4(\zeta_i)$$

For some $\zeta_i, \eta_i \in (t_{i-1}, t_{i+1})$.

Reformulation as a Feasibility Problem

- We seek a numerical solution $\omega = (\omega_0, \ldots, \omega_{N+1})$ such that $y(a) = \alpha = \omega_0, y(t_1) = \omega_1, \ldots, y(b) = \beta = \omega_{N+1}$.
- From formula on previous slide, we obtain a nonlinear system:

$$-\alpha + 2\omega_1 - \omega_2 + h^2 f\left(t_1, \omega_1, \frac{\omega_2 - \alpha}{2h}\right) = 0 \text{ Eqn(1)}$$

$$-\omega_1 + 2\omega_2 - \omega_3 + h^2 f\left(t_2, \omega_2, \frac{\omega_3 - \omega_1}{2h}\right) = 0 \text{ Eqn(2)}$$

$$\vdots$$

$$-\omega_{N-2} + 2\omega_{N-1} - \omega_N + h^2 f\left(t_{N-1}, \omega_{N-1}, \frac{\omega_N - \omega_{N-2}}{2h}\right) = 0 \text{ Eqn(N} - 1)$$

$$-\omega_{N-1} + 2\omega_N - \beta + h^2 f\left(t_N, \omega_N, \frac{\beta - \omega_{N-1}}{2h}\right) = 0 \text{ Eqn(N)}$$

- Let $\Omega_i = \{\omega = (\omega_1, \ldots, \omega_N) | \omega \text{ satisfies the } i\text{th equation}\}$.
- Finding $\omega \in \cap_{k=1}^{N} \Omega_k$ numerically solves the ODE.

Product Space Projections

$P_A(x)$ updates all colored values.

$P_{\Omega_1}(x_1)$	$P_{\Omega_2}(x_2)$	$P_{\Omega_3}(x_3)$	$P_{\Omega_4}(x_4)$	$P_{\Omega_5}(x_5)$	$P_{\Omega_6}(x_6)$
$\underline{x_{1_1}}$	$\underline{x_{2_1}}$	x_{3_1}	x_{4_1}	x_{5_1}	x_{6_1}
$\underline{x_{1_2}}$	$\underline{x_{2_2}}$	$\underline{x_{3_2}}$	x_{4_2}	x_{5_2}	x_{6_2}
x_{1_3}	$\underline{x_{2_3}}$	$\underline{x_{3_3}}$	$\underline{\underline{x_{4_3}}}$	x_{5_3}	x_{6_3}
x_{1_4}	x_{2_4}	$\underline{x_{3_4}}$	$\underline{\underline{x_{4_4}}}$	$\underline{\underline{x_{5_4}}}$	x_{6_4}
x_{1_5}	x_{2_5}	x_{3_5}	$\underline{\underline{x_{4_5}}}$	$\underline{\underline{x_{5_5}}}$	$\underline{\underline{x_{6_5}}}$
x_{1_6}	x_{2_6}	x_{3_6}	x_{4_6}	$\underline{\underline{x_{5_6}}}$	$\underline{\underline{x_{6_6}}}$

$P_B(x)$ averages across rows, updates all values.

$\frac{1}{6}\sum_{j=1}^{6} x_{j_1}$	x_{1_1}	x_{2_1}	x_{3_1}	x_{4_1}	x_{5_1}	x_{6_1}
$\frac{1}{6}\sum_{j=1}^{6} x_{j_2}$	x_{1_2}	x_{2_2}	x_{3_2}	x_{4_2}	x_{5_2}	x_{6_2}
$\frac{1}{6}\sum_{j=1}^{6} x_{j_3}$	x_{1_3}	x_{2_3}	x_{3_3}	x_{4_3}	x_{5_3}	x_{6_3}
$\frac{1}{6}\sum_{j=1}^{6} x_{j_4}$	x_{1_4}	x_{2_4}	x_{3_4}	x_{4_4}	x_{5_4}	x_{6_4}
$\frac{1}{6}\sum_{j=1}^{6} x_{j_5}$	x_{1_5}	x_{2_5}	x_{3_5}	x_{4_5}	x_{5_5}	x_{6_5}
$\frac{1}{6}\sum_{j=1}^{6} x_{j_6}$	x_{1_6}	x_{2_6}	x_{3_6}	x_{4_6}	x_{5_6}	x_{6_6}

Alternative Scheme I: Stacking (Intersections)

$P_A(x)$ updates all colored values.

$P_{\Omega_1\cap\Omega_4}(x_1)$	$P_{\Omega_2\cap\Omega_5}(x_2)$	$P_{\Omega_3\cap\Omega_6}(x_3)$
$\underline{x_{1_1}}$	$\underline{x_{2_1}}$	x_{3_1}
$\underline{x_{1_2}}$	$\underline{x_{2_2}}$	$\underline{x_{3_2}}$
$\underline{\underline{x_{1_3}}}$	$\underline{x_{2_3}}$	$\underline{x_{3_3}}$
$\underline{\underline{x_{1_4}}}$	$\underline{\underline{x_{2_4}}}$	$\underline{x_{3_4}}$
$\underline{\underline{x_{1_5}}}$	$\underline{\underline{x_{2_5}}}$	$\underline{\underline{x_{3_5}}}$
x_{1_6}	$\underline{\underline{x_{2_6}}}$	$\underline{\underline{x_{3_6}}}$

$P_B(x)$ averages across rows, updates all values.

$\frac{1}{3}\sum_{j=1}^{3} x_{j_1}$	x_{1_1}	x_{2_1}	x_{3_1}
$\frac{1}{3}\sum_{j=1}^{3} x_{j_2}$	x_{1_2}	x_{2_2}	x_{3_2}
$\frac{1}{3}\sum_{j=1}^{3} x_{j_3}$	x_{1_3}	x_{2_3}	x_{3_3}
$\frac{1}{3}\sum_{j=1}^{3} x_{j_4}$	x_{1_4}	x_{2_4}	x_{3_4}
$\frac{1}{3}\sum_{j=1}^{3} x_{j_5}$	x_{1_5}	x_{2_5}	x_{3_5}
$\frac{1}{3}\sum_{j=1}^{3} x_{j_6}$	x_{1_6}	x_{2_6}	x_{3_6}

Alternative Scheme II

$P_A(x)$ updates all colored values.

$P_{\Omega_1}(x_1)$	$P_{\Omega_2}(x_2)$	$P_{\Omega_3}(x_3)$	$P_{\Omega_4}(x_4)$	$P_{\Omega_5}(x_5)$	$P_{\Omega_6}(x_6)$
$\underline{x_{1_1}}$	$\underline{x_{2_1}}$	x_{3_1}	x_{4_1}	x_{5_1}	x_{6_1}
$\underline{x_{1_2}}$	$\underline{x_{2_2}}$	$\underline{x_{3_2}}$	x_{4_2}	x_{5_2}	x_{6_2}
x_{1_3}	$\underline{x_{2_3}}$	$\underline{x_{3_3}}$	$\underline{\underline{x_{4_3}}}$	x_{5_3}	x_{6_3}
x_{1_4}	x_{2_4}	$\underline{x_{3_4}}$	$\underline{\underline{x_{4_4}}}$	$\underline{\underline{x_{5_4}}}$	x_{6_4}
x_{1_5}	x_{2_5}	x_{3_5}	$\underline{\underline{x_{4_5}}}$	$\underline{\underline{x_{5_5}}}$	$\underline{\underline{x_{6_5}}}$
x_{1_6}	x_{2_6}	x_{3_6}	x_{4_6}	$\underline{\underline{x_{5_6}}}$	$\underline{\underline{x_{6_6}}}$

$P_B(x)$ averages across only updated values in rows, updates all.

$\frac{1}{2}\sum_{j=1}^{2} x_{j_1}$	$\underline{x_{1_1}}$	$\underline{x_{2_1}}$	x_{3_1}	x_{4_1}	x_{5_1}	x_{6_1}
$\frac{1}{3}\sum_{j=1}^{3} x_{j_2}$	$\underline{x_{1_2}}$	$\underline{x_{2_2}}$	$\underline{x_{3_2}}$	x_{4_2}	x_{5_2}	x_{6_2}
$\frac{1}{3}\sum_{j=2}^{4} x_{j_3}$	x_{1_3}	$\underline{x_{2_3}}$	$\underline{x_{3_3}}$	$\underline{x_{4_3}}$	x_{5_3}	x_{6_3}
$\frac{1}{3}\sum_{j=3}^{5} x_{j_4}$	x_{1_4}	x_{2_4}	$\underline{x_{3_4}}$	$\underline{x_{4_4}}$	$\underline{x_{5_4}}$	x_{6_4}
$\frac{1}{3}\sum_{j=4}^{6} x_{j_5}$	x_{1_5}	x_{2_5}	x_{3_5}	$\underline{x_{4_5}}$	$\underline{x_{5_5}}$	$\underline{x_{6_5}}$
$\frac{1}{2}\sum_{j=5}^{6} x_{j_6}$	x_{1_6}	x_{2_6}	x_{3_6}	x_{4_6}	$\underline{x_{5_6}}$	$\underline{x_{6_6}}$

Examples

Unless otherwise specified:

- $x_0 = (\omega, \ldots, \omega) \in R^{N \times N}$ where $\omega_i = \alpha + \frac{i(\beta-\alpha)}{N+1}, i = 1, \ldots, N$ matches the affine function satisfying the boundary values.
- $N = 21$
- We compute the error via the L_2 norm:

$$\epsilon := \frac{b-a}{N+1} \sum_{k=1}^{N} |\omega_k' - \omega_k|^2.$$

  - When ω_k' is the value of the true solution at $x_k = a + \frac{k(b-a)}{N+1}$ and ω_k represents the solution of the finite difference problem at x_k calculated using Newton's method, ϵ measures the error between the true solution and the approximate solution.
  - We expect this error to decrease as N is increased.

Example: $y'' = \frac{1}{8}(32 + 2x^3 - yy')$

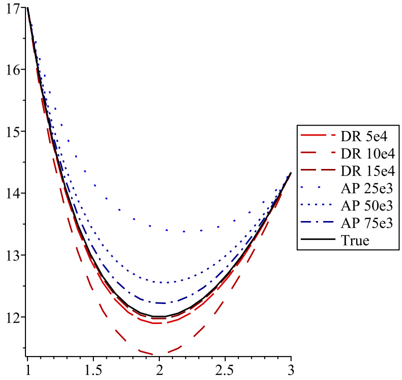

(a) True and approximate solutions

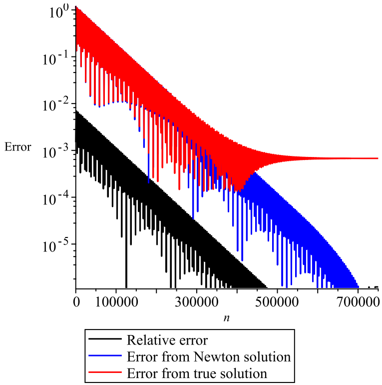

(b) Error for DR iterates

Figure: Convergence behavior for a polynomial Example.

Example: $y'' = \frac{1}{8}(32 + 2x^3 - yy')$

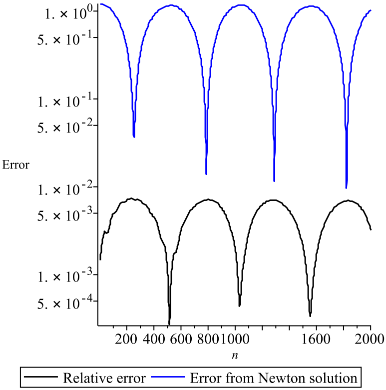

(a) DR

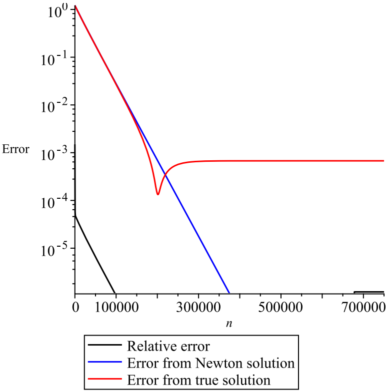

(b) AP

Figure: Convergence behavior for a polynomial example.

Examples: ($y'' = -|y|$) and ($y'' = 0$ if $x < 0$ and y otherwise)

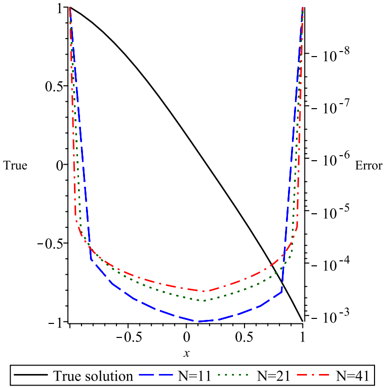

Figure: True solutions (left axis scale) and effect of partition size on error between true solution and estimate by Newton (right axis scale) for Examples **??** (left) and **??** (right).

Example: $y'' = 0$ if $x < 0$ and y otherwise

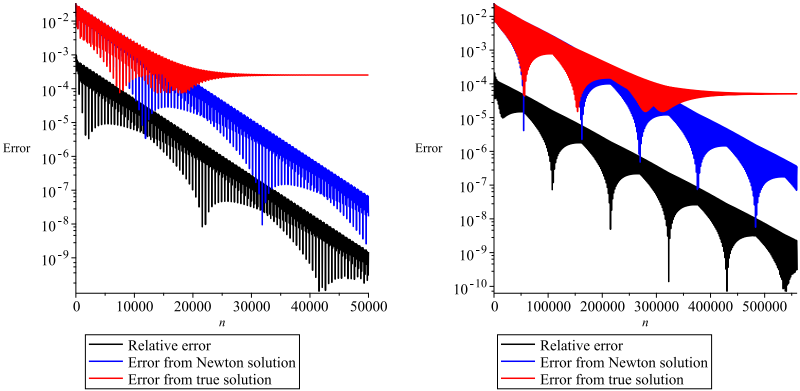

Figure: Effect of N on DR convergence: N=11 (left), N=21 (right)

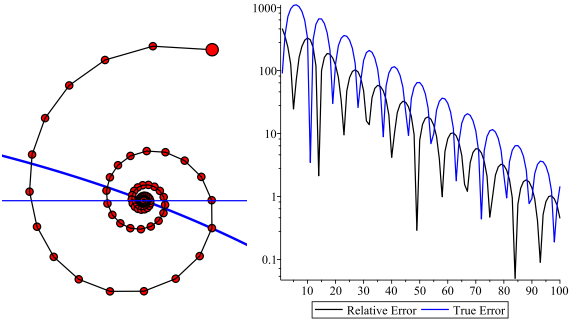

Figure: Relative error and error from true solution for converging DR iterates for an ellipse and line.

- Behavior is consistent with other contexts
- Here the line is the analog of our diagonal set B (**??**), and so at right we report $\|P_L x_{n+1} - P_L x_n\|_2$
- The similarities to Figure 23 are unmistakable.

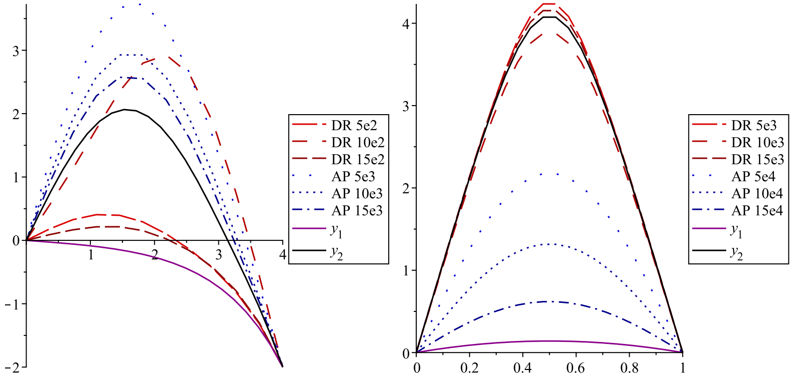

Figure: DR and AP may converge to two different solutions from the same starting point: at left an absolute value problem, at right an exponential problem.

Example $y'' = -|y|$

Method/Start λ	.01	.1	.5	1	2	3	4	5	6	7	8	9
Newton N=11	2	2	2	2	2	2	2	2	2	2	2	2
DR N=11	1	1	2	2	2	2	1	1	1	1	1	1
AP N=11	1	1	2	2	2	2	2	2	2	2	2	2
Newton N=21	2	2	2	2	2	2	2	2	2	2	2	2
DR N=21	1	1	2	2	2	S	S	S	S	2	2	2
AP N=21	1	1	2	2	2	2	2	2	2	2	2	2
Method/Start λ	-.01	-.1	-.5	-1	-2	-3	-4	-5	-6	-7	-8	-9
Newton N=11	1	1	1	1	1	1	1	1	1	1	1	1
DR N=11	1	1	1	1	1	1	1	1	1	1	1	1
AP N=11	1	1	1	1	1	1	1	1	1	1	1	1
Newton N=21	1	1	1	1	1	1	1	1	1	1	1	1
DR N=21	1	1	1	1	1	S	S	S	S	2	2	2
AP N=21	1	1	1	1	1	1	1	1	1	1	1	1

Table: Sensitivity to starting point for an absolute value problem: 1 or 2 indicate the method converged to y_1 or y_2 while S indicates the method appeared stuck after 5E5 iterates. Column headers of λ indicate functions which matched the boundary values and were $\lambda\chi_{(0,4)}$ everywhere else.

Example: $y'' = -|y|$

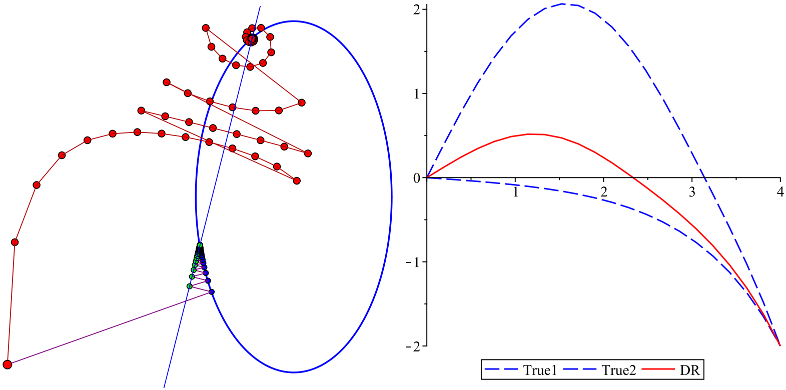

Figure: Left: DR started sufficiently far from two feasible points may converge to the farther of the two while AP converges to the nearer. Right: for Example **??** after 5E5 iterates DR appears stuck for some starting points.

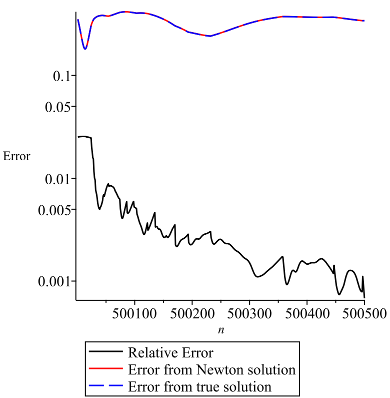

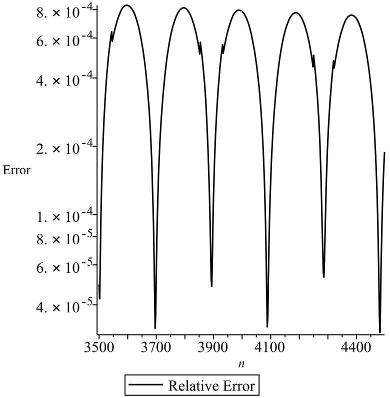

Figure: Left: stuck DR. Right: relative error tends toward a pattern other than smooth oscillation.

Example: $y'' = -|y|$

Method / Start λ	-1	0	1	2	3	4	5	6	7
Newton N=11	1	1	1	1	2	D	D	D	D
DR N=11	1	1	1	2	2	2	2	2	2
AP N=11	1	1	1	1	2	2	2	S	S
Newton N=21	1	1	1	1	2	D	D	D	D
DR N=21	1	1	1	2	2	2	2	2	2
AP N=21	1	1	1	1	2	2	2	2	S

Table: Sensitivity to starting point for Example **??**: $1, 2$ indicates the method converged to y_1, y_2 respectively while "D" and "S" respectively indicate the method diverged or appeared stuck. Column headers of λ indicate functions which matched the boundary values and were $\lambda\chi_{(0,1)}$ everywhere else.

Example: Heaviside

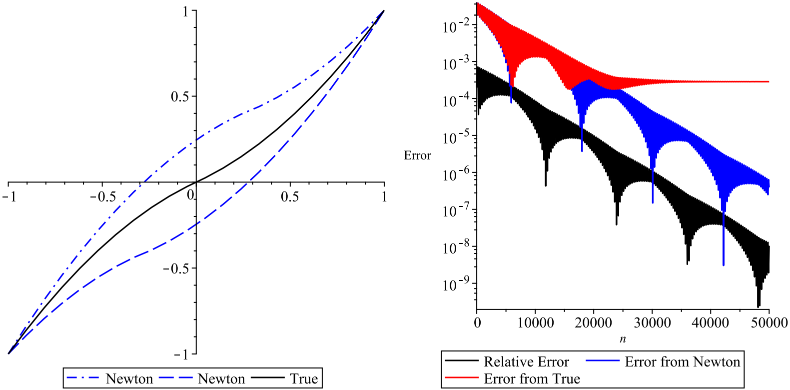

Figure: Newton's Method may cycle for certain starting points in a Heaviside problem (left) while DR converges (right).

Examples: Summary

	DR 1E−1	AP 1E−1	DR wave	DR $\frac{\text{Error}}{\text{Relative}}$	AP $\frac{\text{Error}}{\text{Relative}}$	True error
Ex ?? N=11	9E3	4E3	142	44	2E3	3.4E−3
N=21	129E3	60E3	516	155	26E3	6.7E−4
Ex ?? N=11	18E3	9E3	198	63	4E3	4.7E−4
N=21	247E3	102E3	715	227	53E3	1.3E−4
Ex ?? N=11	9E3	4E3	138	43	2E3	2.5E−4
N=21	117E3	58E3	500	155	25E3	5.1E−5
Ex ?? N=11	2E3	1E3	65	19	4E2	3.1E−3
N=21	25E3	12E3	230	67	5E3	6.2E−4
Ex ?? N=11	16E3	8E3	184	57	34E2	2.6E−5
N=21	208E3	104E3	670	211	46E3	5.1E−6
Ex ?? N=11	1E3	4E2	41	12	1E2	1.4E−3
N=21	11E3	5E3	149	46	2E3	2.9E−4

Table: A summary of experimental results from all examples.

Lessons

- The poor tradeoff in convergence rate for finer partitions suggests some modifications to the method for solving real world problems.
    - One such modification is to begin with a coarse partition and increase the fineness over time.
    - Another is to simply switch to a more traditional solver once sufficient proximity to the true solution is suspected from analysis of the relative error.
- The impressive stability of the Douglas-Rachford method relative to more traditional methods is consistent with previous findings in the application of these methods to finding the intersections of analytic curves [?LSS]
- This property and its unique suitability for parallelization make it an ideal candidate for employment in settings where traditional solvers fail.

This work is dedicated to the memory of Jonathan Borwein: our advisor, mentor, and friend.

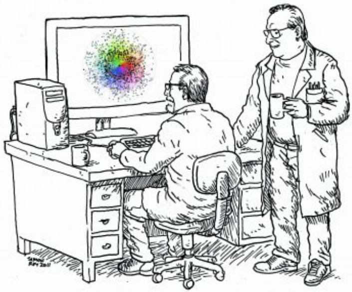

"Sometimes it is easier to see than to say."

Image drawn by Simon Roy at request of Jon and Veselin Jungic:

(http://jonborwein.org/2016/08/jon-borwein-a-friend-and-a-mentor/)

Thanks for listening!

References I

[1] F.J. Aragón, J.M. Borwein. "Global convergence of a non-convex Douglas-Rachford iteration," *Journal of Global Optimization* 57 (2013), Issue 3, 753769.

[2] F.J. Aragón Artacho, J.M. Borwein, and M.K. Tam. "Recent results on Douglas-Rachford methods for combinatorial optimization problems," *Journal of Optimization Theory and Applications*, **163** (2014) 1-30.

[3] F.J. Aragón Artacho, J.M. Borwein, M.K. Tam. "Douglas-Rachford feasibility methods for matrix completion problems," *ANZIAM Journal*. **55(4)** (2014) 299-326.

[4] F.J. Aragón Artacho, R. Campoy: "Solving graph coloring problems with the Douglas-Rachford algorithm." Submitted December 2016, arXiv: `https://arxiv.org/pdf/1612.05026v1.pdf`

[5] David H. Bailey and Jonathan M. Borwein, "Experimental computation as an ontological game changer: The impact of modern mathematical computation tools on the ontology of mathematics." In *Mathematics, Substance and Surmise: Views on the Meaning and Ontology of Mathematics*, Springer, 25-67.

[6] H.H. Bauschke and P.L. Combettes, *Convex Analysis and Monotone Operator Theory in Hilbert Spaces*, second edition, Springer, 2017.

[7] H.H. Bauschke, P.L. Combettes, and R.D. Luke, "Phase retrieval, error reduction algorithm, and Fienup variants: a view from convex optimization", *J. Opt. Soc. Amer. A* **19** (2002), 1334–1345.

[8] Heinz H. Bauschke and Walaa M. Moursi, "On the Douglas-Rachford algorithm," `http://arxiv.org/pdx/1604.04603.pdf`.

[9] J. Benoist, "The Douglas-Rachford Algorithm for the Case of the Sphere and the Line," *Journal of Global Optimization*: 63 (2015), 363-380.

[10] J.M. Borwein. "The Life of Modern Homo Habilis Mathematicus: Experimental Computation and Visual Theorems." *Tools and Mathematics,* 23-90, in *Mathematics Education Library*, vol. 347, Springer, 2016.

References II

[11] J.M. Borwein, S.B. Lindstrom, B. Sims, M. Skerritt and A. Schneider, "Dynamics of the Douglas Rachford Method for Ellipses and p-Spheres," to appear in *Set Valued Variational Analysis*, available at `https://arxiv.org/abs/1610.03975` .

[12] J.M. Borwein and B. Sims, The Douglas-Rachford algorithm in the absence of convexity, Fixed-Point Algorithms for Inverse Problems in Science and Engineering, Springer Optimization and its Applications: 49 (2011), 93-109.

[13] J.M. Borwein, and M.K. Tam, "A cyclic Douglas–Rachford iteration scheme," Journal of Optimization Theory and Applications, **160** (2014), 1–29.

[14] J.M. Borwein and Matthew K. Tam. "Reflection methods for inverse problems with applications to protein conformation determination," Springer volume on the CIMPA school [?GeneralizedNashEquilibriumProblems, ?BilevelprogrammingandMPEC], New Delhi, India, Dec. 2012.

[15] Haim Brezis, *Functional Analysis, Sobolev Spaces and Partial Differential Equations*, Springer (2011).

[16] R.L. Burden, D.J. Faires, and A.M. Burden, *Numerical Analysis*, Cengage Learning, 2016.

[17] J. Douglas and H.H. Rachford, "On the numerical solution of the heat conduction problem in 2 and 3 space variables," *Transactions of the AMS* **82** (1956), 421439.

[18] F. Deutsch, Rate of convergence of the method of alternating projections, in B. Brosowski and F. Deutsch (eds), *Parametric Optimization and Approximation*, Birkhäuser, Basel, 1983, pp96–107.

[19] Asen L. Dontchev, private communication.

[20] J. Douglas and H.H. Rachford, "On the numerical solution of the heat conduction problem in 2 and 3 space variables," *Transactions of the AMS* **82** (1956), 421439.

References III

[21] V. Lakshmikantham and D. Trigiante, *Theory of Difference Equations - Numerical Methods and Applications*, Marcel Dekker, 2002, ppx+300.

[22] S.B. Lindstrom, B. Sims, and M.P. Skerritt, "Computing Intersections of Implicitly Specified Plane Curves," to appear in Journal of Nonlinear and Convex Analysis.

[23] P.L. Lions and B. Mercier, "Splitting algorithms for the sum of two nonlinear operators," *SIAM Journal on Numerical Analysis,* **16** (1979), 964979.

[24] Tristan Needham, *Visual complex analysis*, Clarendon Press, Oxford, 1997, ppxiii+612.

[25] Tim Stellmach - SVG version of "Sudoku-by-L2G-20050714.gif," a Sudoku layout generated by the GNU program Su Doku Solver and contributed in the public domain by Lawrence Leonard Gilbert. Created in Inkscape., Public Domain, `https://commons.wikimedia.org/w/index.php?curid=1167411`

[26] G. Pierra "Decomposition through formalization in a product space," Math. Programming, **28** (1984), 96115.